Bulletin of Engineering Geology and the Environment (2019) 78:5977–5989
https://doi.org/10.1007/s10064-019-01493-3

ORIGINAL PAPER

Comparative analysis of rockmass characterization techniques for the stability prediction of road cut slopes along NH-44A, Mizoram, India

Sahil Sardana[1] · A. K. Verma[2] · Anand Singh[1] · Laldinpuia[3]

Received: 8 October 2018 / Accepted: 25 February 2019 / Published online: 22 March 2019

Abstract
The network of roads in hilly areas plays an important role in the socio-economic development of any country. Instability in road cut slopes is the most critical and common problem in the Northeast region of India. We conducted rockmass characterization of thirteen slopes from three regions, namely Lengpui, Phunchawng and Aizawl Zoo areas near the Aizawl city, on the basis of rock mass rating (*RMR*), geological strength index (*GSI*), kinematic analysis, and various slope mass rating techniques. Wedge failure was observed to be prominent in these regions, though some other modes of failure were present at the site. The stability of road cut slopes was found to vary from partially stable to completely unstable with regard to slope mass rating (*SMR*), Chinese slope mass rating (*CSMR*) and the continuous slope mass rating (*CoSMR*). A comparative analysis was also carried out among the findings of various rockmass characterization techniques to predict the stability of the road cut slopes along NH-44A highway.

Keywords Road cut slopes · Rock mass rating · Kinematic analysis · Slope mass rating · Aizawl · Rockmass characterization

Introduction

Rock slope plays an important role in the stability of surface structures. The instability of a rock slope may be a significant hazard, giving rise to maintenance and property damages, injuries, fatalities and economic losses. Rockfall and landslide create severe problems, especially during the rainy season in the Northeast region of India. In April 2017, a small-scale landslide disrupted traffic for one to two days on the Lengpui airport highway. This is the only highway that connects the Aizawl city to the airport, and is known as a lifeline for Aizawl. The engineering rockmass classification system is the backbone of the empirical design approach for designing support measures. On the basis of rock mass classification systems, the empirical approach has gained popularity because of its simplicity and its ability to manage uncertainty (Anbazhagan et al. 2017). The rock mass classification system provides guidelines and quantitative data that can modify the interpretation of rockmass from structural and inherent guidelines (Pantelidis 2009; Liu and Chen 2007) by an arithmetic algorithm. Hack (2002) explained that the rockmass classification considers the parameters that are associated with intact rock strength, geometry of slope, shear strength along discontinuities, and block size or discontinuity spacing. Some of these parameters have very little influence on slope stability. As an outgrowth, an engineering rock mass classification system should be used for initial planning or during the engineering design stage. Many researchers have carried out stability assessments using slope mass rating techniques (Basahel and Mitri 2017; Kundu et al. 2017; Azarafza et al. 2017; Siddique et al. 2015), an artificial neural network method (Verma et al. 2016), a limit equilibrium method (Kumar et al. 2017; Zheng et al. 2017) and other techniques (Yardimci and Karpuz 2018; Verma et al. 2018a,

✉ Sahil Sardana
sahilsardana.ymca@gmail.com

[1] Department of Mining Engineering, Indian Institute of Technology (Indian School of Mines), Dhanbad, Jharkhand 826004, India

[2] Department of Mining Engineering, Indian Institute of Technology (Banaras Hindu University), Varanasi, Uttar Pradesh 221005, India

[3] Department of Geology, Pachhunga University College, Aizawl, Mizoram 796001, India

2018b; Kaya 2017; Sarkar et al. 2016; Singh and Verma 2007). In the field of mining, the stability of tunnels (Verma and Singh 2010), overburden slopes and stability in soil slopes (Singh et al. 2018) have been assessed by many researchers.

In this study, rockmass classification has been carried out to estimate the instability in thirteen road cut slopes along the airport highway NH-44A near Aizawl city. The stability condition for each slope has been identified using the rock mass rating (*RMR*), geological strength index (*GSI*), and various slope mass rating (*SMR*) techniques along with kinematic analysis. The *RMR* method, or geo-mechanics classification system, was first originated at the South African Council of Scientific and Industrial Research (*CSIR*) (Bieniawski 1979). The main purpose of the rockmass classification system is to provide quantitative details and guidelines for engineering design that modifies original descriptions of a geological formation. The *RMR* classification system can be used as a recommendation for selecting appropriate excavation techniques, to forecast standup time, type of rock reinforcements and long-lasting support in tunnels. The *RMR* method can also be used to obtain the susceptibility to landslide of rock slopes, which allows engineers to determine the critical sections of a rock mass that could be prone to failure. Apart from mining, *RMR* can also be used for designs related to rippability, weatherability, boreability, foundations, and dredging. Advantages of *RMR* include its ease of application, potential to evaluate rock quality across the surface as well as underground operations in every part of a site, and its use in characterizing empirical relationships, which includes Hoek-Brown failure criterion (Marinos et al. 2007). The *RMR* method has disadvantages in the evaluation of weak rockmass, which can be overcome by the *GSI* technique. It is broadly used for quick and qualitative assessment of rockmasses. A graph for obtaining the *GSI* was proposed by Hoek and Brown (1997) considering the two parameters, i.e. rock parameters and condition of discontinuities. The discontinuities are distributed into five surface conditions which are very good, good, fair, poor and very poor. *GSI* is an index of characterizing rock masses and is not meant to replace any other classification system (Chaurasia et al. 2017). The main function of *GSI* is to calculate the rock mass strength using Hoek-Brown failure criteria. It was quantified by Somnez and Ulusey (Sonmez and Ulusay 2002) to obtain more precise values. The modified *GSI* chart includes five categories of structure rating (*SR*) and five categories of surface condition rating (*SCR*). In the present study, a modified *GSI* chart has been used for rockmass classification.

The stability of the road cut slope was also assessed by various *SMR* techniques such original *SMR* (Romana 1985), Chinese *SMR* (Chen 1995) and continuous *SMR* (Tomás et al. 2007). *SMR* was developed by Romana (1985), in which four correction parameters were added in the basic *RMR*. Out of four, three correction parameters directly depend on the relationship between the discontinuities and fourth parameter depends on the slope excavation method (Goel and Singh 2011). Initially *SMR* was developed only for topple and planar failure; ratings for wedge failure were added later by Anbalagan (1992). The consequence of weathering on slope stability for a long time cannot be evaluated by this classification system. It is always wise to investigate *SMR* against an adjoining stable rock mass prior to applying it to distressed rock slopes (Azzuhry 2016). Chinese slope mass rating (*CSMR*) was developed by Chen (1995) with the inclusion of two coefficient in the original *SMR* equation. These two coefficients account for the effects of slope height and the type of discontinuity in the slope. The slope height coefficient is only applicable for slopes greater than 80 m in height, whereas discontinuity coefficient considers long weak seams, continuous bedding plane and intact bedding planes. The scoring of *SMR* and *CSMR* are discrete functions; to make them continuous functions, continuous slope mass rating (*CoSMR*) was proposed by Tomas et al. (Tomás et al. 2007). *CoSMR* is the amendment of *SMR* by a continuous function. The *CoSMR* method replaced the discrete correction factors proposed by Romana (1985) with a continuous function. A detailed investigation should be carried out when the *SMR* value is less than 40. The limitation of *SMR* is its application in the open cast mines, as hefty blasting forms new fractures in the rock and the extent of the cut slope also enlarges. The *SMR* rating classifies slopes in five stability classes, which are completely unstable (<20), unstable (20–40), partially stable (40–60), stable (60–80) and completely stable (80–100).

Study area

Aizawl is the largest city as well as the capital city of Mizoram state, India. Mizoram is one of the easternmost parts of India, bordered by Bangladesh to west and south-west, Assam to the north, Manipur to north-east and Burma to the east and south-east. The city is situated at the northern part of the tropic of cancer in the north of Mizoram and is located at 1132 m (3715 ft.) above sea level, with the Tuirial river basin to its east and the Tlawng river basin to its west. The city has a total population of 404,054 (2011 census) and has a total area of 3576 sq. km. Aizawl is also one of the seven sister north-eastern mountainous states of India and is located from latitude 23°18′17” N to 24°25′16” N and longitude 92°37′ 03″ E to 93°11′45″ E in the northern part of the state. Aizawl district falls under Survey of India toposheet no. 83D/15, 83D/16, 84A/10, 84A/11 and 83H/4. The whole

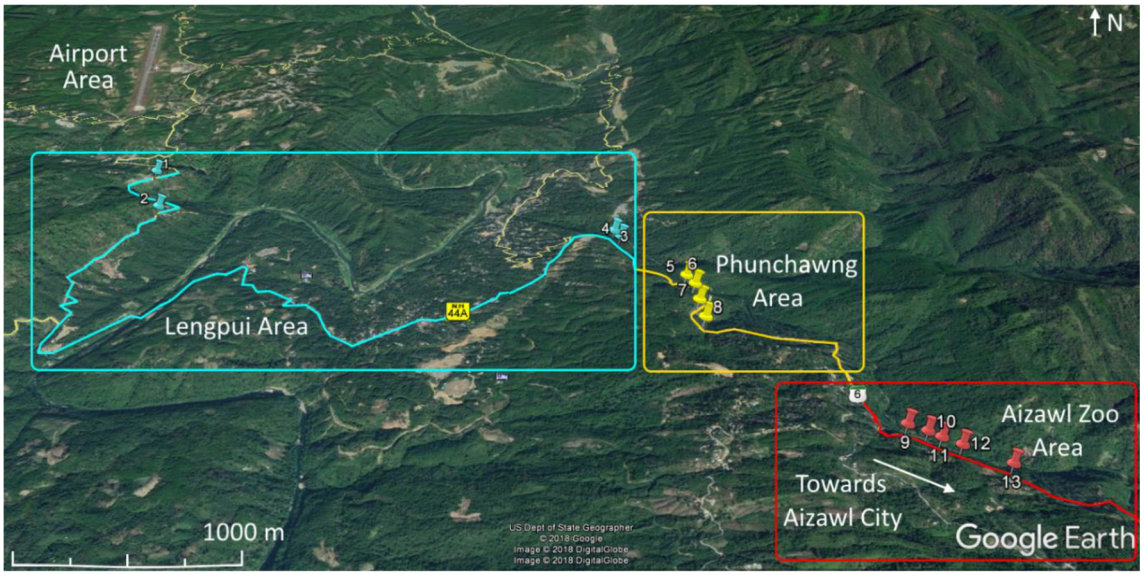

Fig. 1 Modified satellite Imaginary of NH-44A airport road showing the location of Lengpui, Phunchawng and Aizawl Zoo regions

district is under the impact of monsoon, with an ordinary rainfall of 3155.3 mm annually.

Location of the area

In this study, thirteen slopes from three regions were studied, from the Airport to Aizawl city along NH-44A (Fig. 1). The three regions, namely Lengpui area, Phunchawng area and Aizawl Zoo area, comprise four slopes (L1-L4), four slopes (L5-L8) and five slopes (L9-L13) respectively (Table 1). Mostly sandstone-shale or siltstone-shale intercalation was observed in these regions. During the field survey, the height of two slopes, L-1 and L-12, were measured at 30 m and 31 m, respectively, and for the remaining slopes, the slope height varyied from 5 m to 15 m in Lengpui, Phunchawng and Aizawl Zoo region. The site photographs of the slopes from the three regions are shown in Fig. 2.

Geology of the area

The conventional geology of the area shows recurrent observation of Neogene sedimentary rocks of Tipam and Surma group formation. The entire Aizawl city includes top and middle Bhuban dispositions of the Surma group of rocks (Kesari 2011). This group of rocks embraces alternate beds of shale, siltstone, sandstone and mudstone of diverse thicknesses. Sandstones are hard, compact and stable, whereas shale beds are brittle as compared to sandstone. They include bands of micaceous-felspathic and weathered sandstone (Lallianthanga and Lalbiakmawia 2013). An arenaceous and argillaceous batch of rocks lies in relatively upper and lower ground, respectively. Reconnaissance traversing from Aizawl to Champhai resulted in the identification of a Barail batch of rocks in and around Champhai subdivision, Aizawl district, and Bhuban in the west.

Barail class comprises the entire eastern part of the state. Lithological dissimilarity between the Barail group and the Bhuban formation lies in the west. Barail batch of rocks incorporates a band of weathered feldspathic, micaceous, smooth, medium-grained sandstone (greywacke) with a little dark grey, compact, fine to medium grained sandstone band. Barail contains a few sedimentary structures like oscillatory ripples and flute casts. Sedimentary formation comprises interfering and straight-forward ripple marks (rhombohedral

Table 1 Detail of road cut slopes along NH-44A on Airport road

S. No.	Studied region	Distance from Airport (in km)	Latitude	Longitude
1	Lengpui (L1-L4)	3.7	23°49'09.00"N to 23° 48'22.97"N	92°37'32.00"E to 92° 39'40.92"E
2	Phunchawng (L5-L8)	13.8	23° 48'01.49"N to 23° 46'52.95"N	92° 39'53.21"E to 92° 39'52.96"E
3	Aizawl Zoo (L9-L13)	16.8	23° 47'48"N to 23° 46'52.95"N	92° 40'54"E to 92° 40'21.42"E

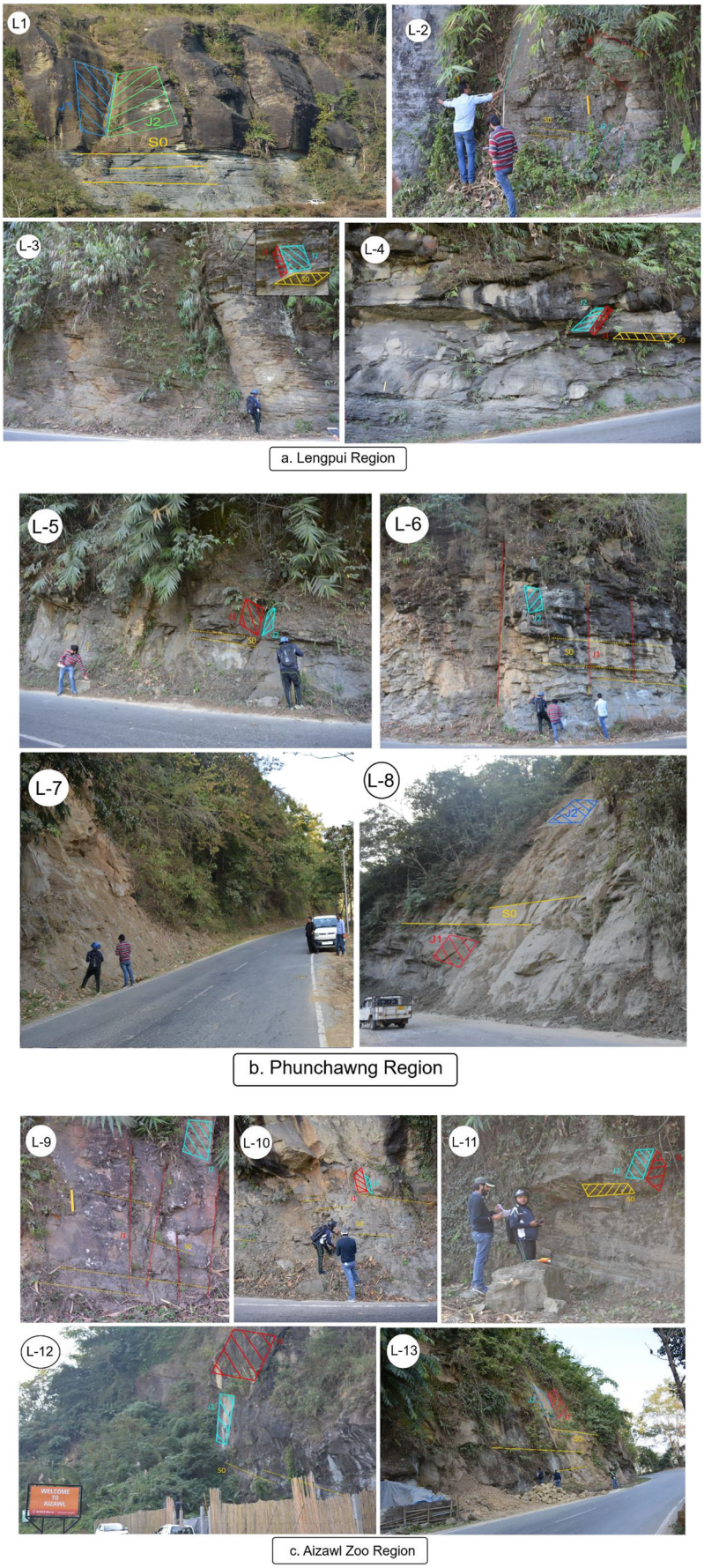

Fig. 2 Field photographs showing joint distribution and different mode of failure for (**a**) Lengpui region from slope L-1 to L-4; (**b**) Phunchawng region from slope L-5 to L-8; (**c**) Aizawl Zoo region from slope L-9 to L13

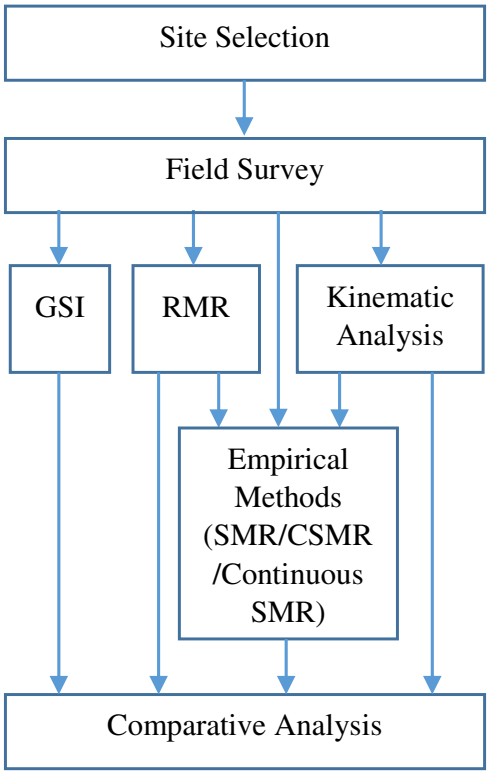

Fig. 3 Methodology used in the study

and linguoid type), ripple drift cross-laminations, wavy/lenticular bedding, flaser bedding, cross stratification, flute casts, grove marks, load casts and convolute laminations. Average strike of bedding is SSW- NNE with dips ranging from 40^0 to 50^0 to both east and west of the state. The rocks in the Barail group have fewer (3^0–15^0) rolling dips and are folded into a vast anticline with its axis trending roughly E-W (Laldinpuia et al. 2014).

Methodology

This paper focuses on the rockmass characterization of the road cut slopes using *RMR*, *GSI* and various *SMR* techniques. The methodology used in the study is shown in Fig. 3 as a flowchart.

An extensive field survey was carried out to assess the qualitative and quantitative factors used in the rockmass characterization. The kinematic analysis, basic *RMR* and quantified *GSI* were evaluated based on the data obtained from site investigation. The various *SMR* valueswere calculated using the empirical formulae by using the basic *RMR*, field data and kinematic analysis. Further, a comparative analysis was carried out using various stability techniques of rockmass characterization.

Results and discussion

As mentioned in the methodology, six different techniques for estimating the slope stability have been used. Kinematic study was done prior to *RMR* and *SMR* of scrutinized slopes to identify the modes of failure.

Stability from basic rock mass rating (RMR_b)

All five parameters were evaluated for the determination of the basic *RMR* for all the thirteen locations. In-situ uniaxial compressive strength (*UCS*) was determined with the help of a Schmidt rebound hammer; its values varied from 25.5 to 41 *MPa* along this stretch. Range and mean value of the in-situ *UCS* for each location is provided in Table 2. Rock quality designation (*RQD*) was determined using volumetric joint count (Jv) (Palmstrom 1982) using Eq. 1. Slope L-1 has big massive rock blocks of approximately 18 m height and had the highest *RQD* rating, which means the rockmass is of excellent quality, whereas rockmass for slopes L-5, L-9 and L-10 have the lowest ratings, indicating poor quality rockmass. The volumetric joint (*Jv*)was obtained by computing the joints in cubic meter volume of a rock mass during the site investigation. Rating of joint spacing, surface condition and ground-water condition were evaluated during the field survey. Only one slope (L-10) has wide joint spacing, four slopes (L-1, L-6, L-7 and L-12) have moderate joints spacing and joints of remaining slopes were observed to be closely spaced. The persistence of the joints varied from 3 to 20 m and the apertures varied from 1 mm to 5 mm. Roughness varied from slightly rough to smooth, and weathering varied from slight to high. Infilling material was observed from soft filling material to none. One out of thirteen slopes (i.e slope L-12) has water flowing conditions, whereas the remaining slopes were found to be completely dry. The basic *RMR* values (Bieniawski 1989) for all the slopes were calculated using Eq. 2. All the slopes except L-1 show fair classification of rockmass and represent category III of basic *RMR* (Table 3).

$$RQD = 115 - 3.3\mathrm{Jv} \tag{1}$$

$$RMR_b = R_{UCS} + R_{RQD} + R_{JS} + R_{JC} + R_{GWC} \tag{2}$$

where RMR_b is the basic *RMR* value, R_{UCS}, R_{RQD}, R_{JS}, R_{JC} and R_{GWC} represent a rating of *UCS*, *RQD*, *JS*, *JC* and *GWC* as per the Bieniawski (1989) Table. *UCS* is uniaxial compressive strength (in MPa); *RQD* is rock quality designation (in %); *JS* is joint spacing (in meters); *JC* is joint condition (in meters), *GWC* is ground-water condition (L/min) and *Jv* is volumetric joint (number of joints per cubic meter).

Table 2 In-situ UCS value calculated by Schmidt rebound hammer on each site

Location	Range (MPa)	Mean (MPa)	Location	Range (MPa)	Mean (MPa)
L-1	39.5–43.0	41.5	L-8	37.5–39.0	38
L-2	33.0–37.5	35	L-9	28.0–35.5	32.5
L-3	28.0–32.5	30.5	L-10	32.5–36.5	34
L-4	32.5–37.5	34.5	L-11	32.0–35.0	33.5
L-5	23.5–27.0	25.5	L-12	32.0–39.0	36.5
L-6	28.0–36.5	31	L-13	28.0–36.5	32.5
L-7	28.0–31.5	30	–	–	–

Stability from geological strength index (*GSI*)

Quantified *GSI* was calculated on the basis of two parameters, i.e. 'structure rating' (*SR*) and 'surface condition rating' (*SCR*). *SR* and *SCR* were evaluated on the basis of field investigation. *SR* is dependent on *Jv* and was calculated by Eq. 3. *SCR* was calculated by addition of roughness, weathering and infilling rating using Eq. 4. All the calculated *GSI* values have been plotted in the quantified *GSI* chart (Sonmez and Ulusay 2002).

$$SR = -17.5\ln(Jv) + 79.8 \quad (3)$$

$$SCR = R_R + R_W + R_I \quad (4)$$

where *SR* is structure rating, *SCR* is surface condition rating, R_R, R_W, and R_I represents ratings for roughness, weathering and infilling, respectively.

The quantified *GSI* results show that slope L-1 has a blocky structure with good surface condition, three slopes (L-8, L-12 and L-13) have a very blocky structure with fair surface condition and the remaining slopes have a blocky/disturbed structure with surface condition varying from poor to good. The plotted value of quantified *GSI* for Lengpui area, Phunchawng area and Aizawl Zoo area are shown in Fig. 4. Quantified *GSI* values were found ranging from 41 to 58 for the Lengpui region, 29 to 39 for the Phunchawng region and 28 to 44 for the Aizawl Zoo region. Quantified *GSI* value of location L-1 was observed to be higher than other roadcut slopes due to massive sandstone blocks on the underlying shale.

Kinematic analysis

The potential modes of failure in all thirteen roadcut slopeswas assessed by kinematic analysis using DIPS 6.0 (Rocscience Inc. 2010). A stereograph was plotted for each slope providing joint input parameters such as joint (J1 and J2), bed (*S0*), slope (*SL*) orientations and internal friction angle (ϕ) (Fig. 5). All potential modes of failure (planar, wedge and topple) were found in the kinematic analysis. Wedge failure was found to be prominent in the Lengpui and Phunchawng regions whereas, for the Aizawl Zoo region, both planar and wedge were prominent in the kinematic analysis. The stereograph plots of the Lengpui region show wedge failure for two slopes (L-1 and L-3) and toppling for two

Table 3 Rating of parameters involved in RMR determination (Bieniawski 1979)

Location	UCS	RQD	Joint Spacing	Surface Condition					Ground Water Condition	RMR
				Persistence	Aperture	Roughness	Weathering	Infilling		
L-1	4	20	10	1	1	3	3	6	15	63
L-2	4	17	8	2	1	3	3	6	15	59
L-3	4	13	8	2	1	3	3	6	15	55
L-4	4	17	8	2	1	3	1	6	15	57
L-5	4	8	8	2	0	3	1	2	15	43
L-6	4	13	10	2	0	3	1	2	15	50
L-7	4	17	10	2	1	3	3	2	15	57
L-8	4	17	8	1	0	3	3	2	15	53
L-9	4	8	8	2	0	3	3	2	15	45
L-10	4	8	15	2	0	3	1	2	15	50
L-11	4	17	8	2	0	3	3	2	15	54
L-12	4	17	10	1	1	3	5	2	4	47
L-13	4	17	8	2	0	3	5	2	15	56

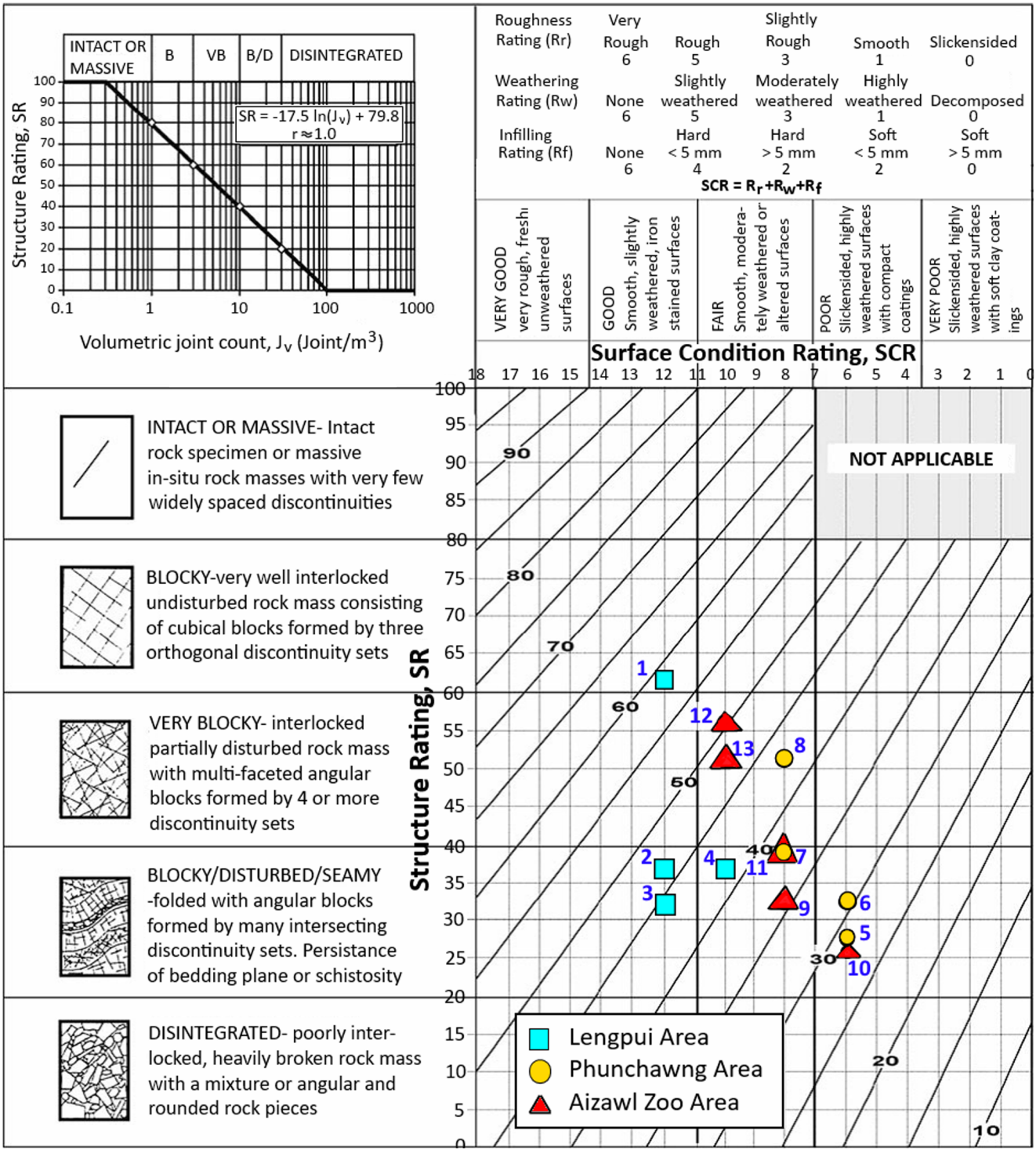

Fig. 4 Calculated *GSI* values mapped on the *GSI* chart provided by Sonmez and Ulusay (2002)

slopes (L-2 and L-4) along with wedge failure. In the Phunchawng region, L-5 and L-6 show only wedge failure, L-7 shows topple and L-8 shows all three types of failure. In the third region, all the slopes show potential for both planar and wedge failure except slope L-11. Slope L-11 shows only topple failure and two slopes, L-12 and L-13, show all three types of failures. The stereograph plots of all the slopes of Lengpui, Phunchawng and Aizawl Zoo regions are shown in Fig. 5a, b and c respectively. The details of input parameters and the types of failure observed in the kinematic analysis for all slopes are provided in Table 4. The various modes of failure have been observed during the field survey. The wedges which have been formed can be seen in the site photographs of slopes L-1, L-3 to L-6, L-10 and L-11. Similarly, planar failure can be seen in site

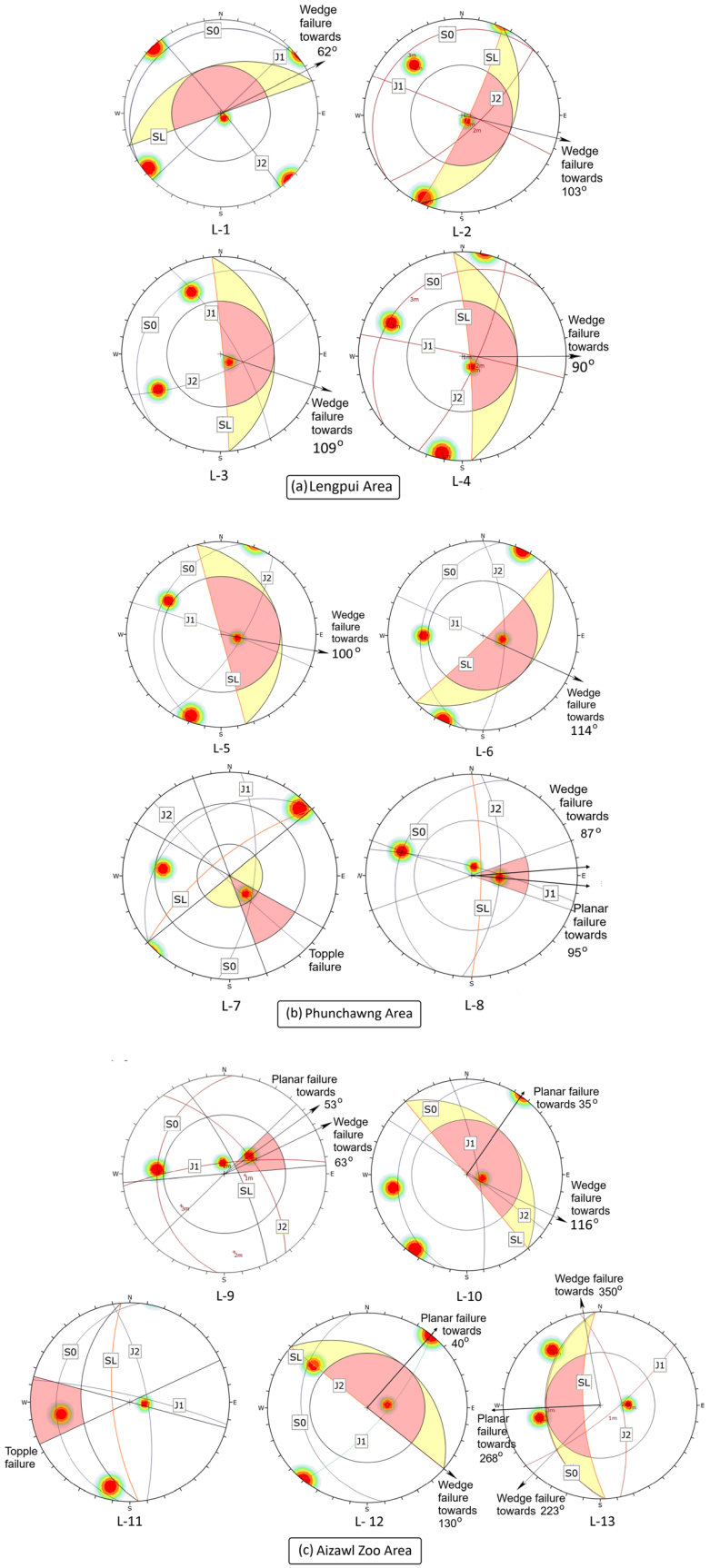

Fig. 5 Stereographic projection of road cut slopes for (**a**) Lengpui area; (**b**) Phunchawng area; (**c**) Aizawl Zoo area along NH-44A

Table 4 Modes of failure observed in the kinematic analysis along NH-44A

Location	Slope No.	Joint Set (Dip/Dip-direction)			Slope Orientation (deg.)	Friction Angle (deg.)	Kinematic Feasibility (%)	Type of Failure
		J1	J2	S0				
Lengpui	L-1	89/135	87/52	7/328	90/340	36	13.33	W
	L-2	86/24	71/137	9/320	82/115	35	17.17	W, T
	L-3	72/60	70/155	14/313	87/85	33	13.34	W
	L-4	87/12	74/115	15/319	82/85	34	22.22	W, T
Phunchawng	L-5	86/20	67/123	20/283	90/75	26	23.81	W
	L-6	90/25	64/90	24/281	85/135	30	16.67	W
	L-7	64/96	85/225	26/319	75/320	34	20	T
	L-8	80/15	60/95	20/290	80/90	33	13.33	P, W, T
Aizawl Zoo	L-9	77/353	56/53	23/274	75/65	28	21.43	P, W
	L-10	87/35	76/80	19/283	90/50	30	13.33	P, W
	L-11	82/13	70/80	17/276	70/265	32	13.33	T
	L-12	70/130	90/40	23/261	90/40	30	26.67	P, W, T
	L-13	75/140	65/78	32/268	70/267	31	14.29	P, W, FT

where *P*: Planar failure; *W*: Wedge failure; *T*: Topple failure; *FT*: Flexural topple failure

photographs of slopes L-8, L-10 and L-11 (Fig. 2). The results of kinematic analysis support the modes of failure observed during the field survey.

Stability from slope mass rating (*SMR*)

Slope mass rating is a significant extension to the RMR_b for preliminary assessment of rock slopes; its values range from 0 to 100. *SMR* is derived from basic *RMR* by incorporating adjustment factors derived from slope-joint relationships and factors derived from the method of excavation. On the basis of the mode of failure, *SMR* values for each slope were calculated as per Eq. 5 (Romana 1985) given below.

$$SMR = RMR_b + (F_1 \times F_2 \times F_2) + F_4 \tag{5}$$

where RMR_b is basic rock mass rating obtained according to the Bieniawski (1989), F_1; F_2, and F_3 are adjustment factors which can be evaluated on the basis of the relationship among discontinuities; F_4 is evaluated on the basis of excavation method. In this paper, the value of F_4 has been taken as '-8' to consider the worst case scenario, i.e. poor blasting for excavation.

The results show that the stability class of various slopes varied from III (partially stable) to V (completely unstable) for all three studied regions. Each slope has been scored depending on the modes of failure. In the Lengpui region, *SMR* rating shows that the slopes L-1 and L-2 were found to be partially stable and unstable, respectively, for wedge failure. Slopes L-2 and L-4 were found to be partially stable for toppling failure but completely unstable for wedge failure. The *SMR* score of Phunchawng region shows that slope L-7 was found to be partially stable and the remaining three slopes (L-5, L-6 and L-8) were completely unstable. In the Aizawl Zoo region, all the slopes appear completely unstable either for planar or wedge failure, and unstable for toppling failure (Table 5). For different modes of failure, the *SMR* result shows different stabilities for the slope, such as for slope L-13, wher the slope was partially stable for wedge failure, unstable for toppling failure and completely unstable for planar failure.

Stability from Chinese slope mass rating (*CSMR*)

The *CSMR* (1995) is another discrete slope mass rating technique with the addition of two factors to the equation of the original *SMR*. These two factors are slope height factor (ξ) and discontinuity factor (λ). *CSMR* was calculated from Eq. 6, by modifying Eq. 5.

$$SMR = \xi RMR_b + \lambda(F_1 \times F_2 \times F_2) + F_4 \tag{6}$$

where ξ and λ can be calculated using Eq. 7 and 8.

$$\begin{cases} \xi = 0.57 + 0.43 \times \dfrac{80}{H} & [for\ slope\ height; H > 80m] \\ \xi = 1 & [for\ slope\ height; H \leq 80m] \end{cases} \tag{7}$$

$$\begin{cases} \lambda = 1 & [for\ faults\ of\ long\ weak\ seams\ filled\ with\ clay] \\ \lambda = 0.8\text{–}0.9 & [for\ bedding\ planes\ of\ large\ scale\ joints\ with\ gouge] \\ \lambda = 0.7 & [for\ joints\ of\ tightly\ interlocked\ bedding\ plane] \end{cases} \tag{8}$$

The results show that the *CSMR* (1995) scores were found to be higher than the *SMR* scores, but the slopes represent the same stability classes in both *SMR* and *CSMR* techniques, except for slope L-12 (Table 5). The stability class of slope L-12 for *CSMR* was the same as

Table 5 Rating of parameters for calculation of SMR (1985), CSMR (1995) and CoSMR (2007)

Location	Failure	Slope Mass Rating (SMR)			Chinese Slope Mass Rating (CSMR)			Continuous Slope Mass Rating (CoSMR)		
		Rating	Class	Stability	Rating	Class	Stability	Rating	Class	Stability
L1	W	47.5	III	Partial Stable	49.00	III	Partial Stable	48.94	III	Partial Stable
L2	W	9	V	Complete Unstable	17.40	V	Complete Unstable	5.07	V	Complete Unstable
	T	47.25	III	Partial Stable	48.00	III	Partial Stable	48.08	III	Partial Stable
L3	W	23	IV	Unstable	30.20	IV	Unstable	22.22	IV	Unstable
L4	W	6.5	V	Complete Unstable	19.25	V	Complete Unstable	−4.79	V	Complete Unstable
	T	45.25	III	Partial Stable	46.38	III	Partial Stable	46.06	III	Partial Stable
L5	W	−7	V	Complete Unstable	−7.00	V	Complete Unstable	11.41	V	Complete Unstable
L6	W	18	V	Complete Unstable	18.00	V	Complete Unstable	12.76	V	Complete Unstable
L7	T	45.25	III	Partial Stable	45.63	III	Partial Stable	43.36	III	Partial Stable
L8	P	−6	V	Complete Unstable	4.20	V	Complete Unstable	−8.81	V	Complete Unstable
	W	−15	V	Complete Unstable	−3.00	V	Complete Unstable	−10.84	V	Complete Unstable
	T	41.25	III	Partial Stable	42.00	III	Partial Stable	42.06	III	Partial Stable
L9	P	−5	V	Complete Unstable	3.40	V	Complete Unstable	−8.28	V	Complete Unstable
	W	−23	V	Complete Unstable	−11.00	V	Complete Unstable	−18.29	V	Complete Unstable
L10	P	7	V	Complete Unstable	7.00	V	Complete Unstable	4.10	V	Complete Unstable
	W	33	IV	Unstable	33.00	IV	Unstable	32.19	IV	Unstable
L11	T	24.75	IV	Unstable	24.75	IV	Unstable	22.05	IV	Unstable
L12	P	14	V	Complete Unstable	21.50	IV	Unstable	9.22	V	Complete Unstable
	W	30	IV	Unstable	32.70	IV	Unstable	30.49	IV	Unstable
	T	35.25	IV	Unstable	36.38	IV	Unstable	35.23	IV	Unstable
L13	P	−3	V	Complete Unstable	2.10	V	Complete Unstable	−4.96	V	Complete Unstable
	W	44.4	III	Partial Stable	44.76	III	Partial Stable	42.61	III	Partial Stable
	W	46.65	III	Partial Stable	46.79	III	Partial Stable	46.46	III	Partial Stable
	FT	26.75	IV	Unstable	28.88	IV	Unstable	25.49	IV	Unstable

where *P*: Planar failure; *W*: Wedge failure; *T*: Topple failure; *FT*: Flexural topple failure

SMR in the case of wedge and topple failures, whereas in the planar failure case, it is completely unstable for *SMR* and unstable for *CSMR*. The height of the slope varied from 9 to 30 m in Lengpui, 5 to 15 m in Phunchawng and 9 to 31 m in Aizawl Zoo. So, the value of ξ is considered '1' due to slope heights less than 80 m for slopes in all three regions. λ is considered as 0.7 for slopes L-3, L-4 and L-7, as the joints were tightly interlocked. Slopes L-5, L-6, L-10 and L-11 have a long weak seam along with the bedding plane filled with clay, hence λ is taken as 1. For the remaining slopes, values were considered as 0.8 or 0.9 because of the large scale of bedding joints with a gouge.

Stability from continuous slope mass rating (*CoSMR*)

The equation for continuous *SMR* is the same as the original *SMR* (Goel and Singh 2011). Suggested ratings by Romana (1985) for F_1, F_2, F_3 and F_4 are disjunctive and rely on the judgment of the field expert. So, it requires an experienced person to determine the ratings for the above parameters. Tomas et al. (2007) obtained a continuous function which best fits the disjunctive values of F_1, F_2, and F_3 as given below, and the value of F_4 is taken as the same as in *SMR*.

$$F1 = \frac{16}{25} - \frac{3}{500} tan^{-1}\left(\frac{1}{10}(|A| - 17)\right) \tag{9}$$

$$F2 = \frac{9}{16} - \frac{1}{195} tan^{-1}\left(\frac{17}{100}(B - 5)\right) \tag{10}$$

$$\begin{cases} F3 = -30 + \frac{1}{3} tan^{-1}(C) & [for\ planar\ and\ wedge\ failure] \\ F3 = -13 - \frac{1}{7} tan^{-1}(C - 120) & [for\ topple\ failure] \end{cases} \tag{11}$$

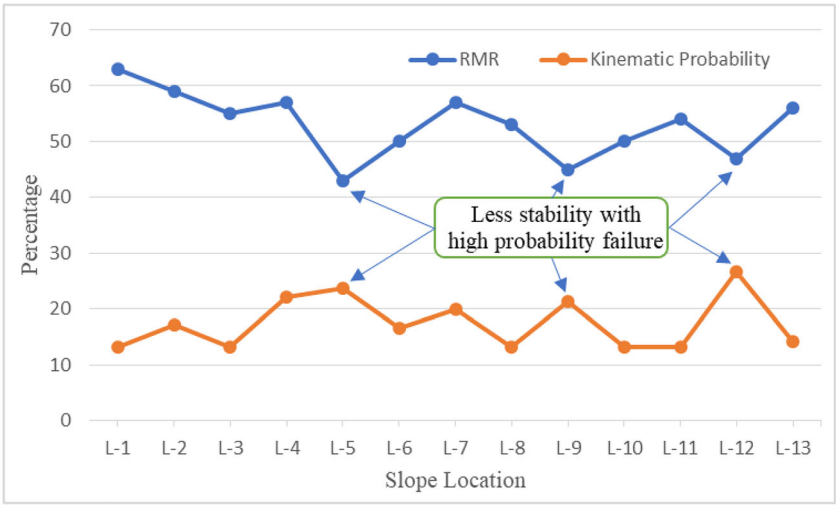

Fig. 6 Comparison between kinematic feasibility and basic rock mass rating

Values of A, B and C can be calculated from the table provided by Romana (1985). The *CoSMR* values were calculated by putting the values of Eq. 9 to 11 in Eq. 5. Results show that the stability class of *CoSMR* is similar to the stability class of *SMR* (Table 5). *CoSMR* gives the maximum vulnerability as its score have been found less than the discrete *SMR* scores for most of the slopes.

Comparative analysis

Comparison between kinematic feasibility and basic *RMR*

Kinematic feasibility was calculated by considering the average of all the critical percentage values for failure (i.e planar, wedge, flexural and direct topple failure) in the kinematic analysis (Table 4). Calculated values of kinematic feasibility for each slope were compared with basic *RMR* values (Fig. 6) to identify the relation between them. The range of kinematic feasibility and rating of RMR_b varyied from 13.33% to 26.67% and 43 to 63, respectively, for all the cut slopes along this highway. It was found that four slopes, L-4, L-5, L-9 and L-12, show the kinematic feasibility greater than 20%, out of which three slopes have RMR_b scores less than 50. L-4 is the only slope which has both high RMR_b and high kinematic feasibility. The comparison of these two parameters for the remaining nine slopes shows that these slopes have high RMR_b with low kinematic feasibility (Fig. 6). The comparative analysis of kinematic feasibility and RMR_b concluded that a slope with lower quality of rockmass may have a high kinematic feasibility.

Comparison between predicted *GSI* (GSI_P) and calculated *GSI* (GSI_C)

In this paper, the *GSI* has been calculated using the quantified *GSI* chart provided by Sonmez and Ulusay (2002). The value

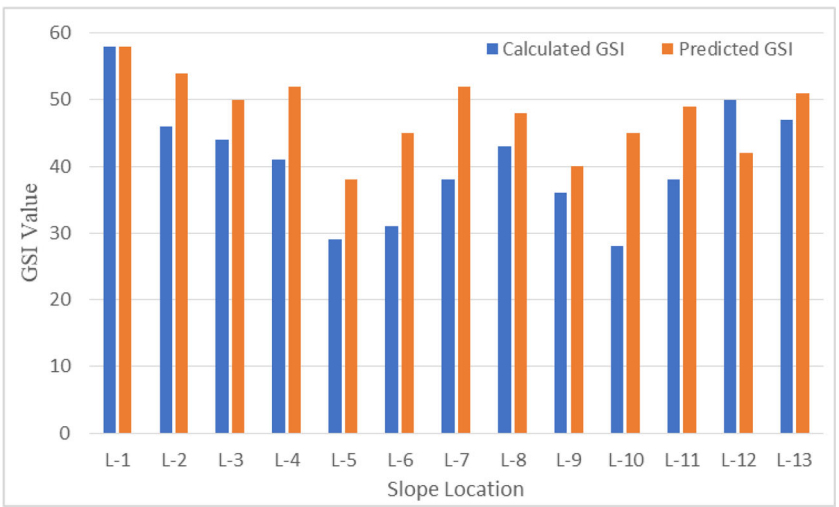

Fig. 7 Comparison between predicted *GSI* and calculated *GSI*

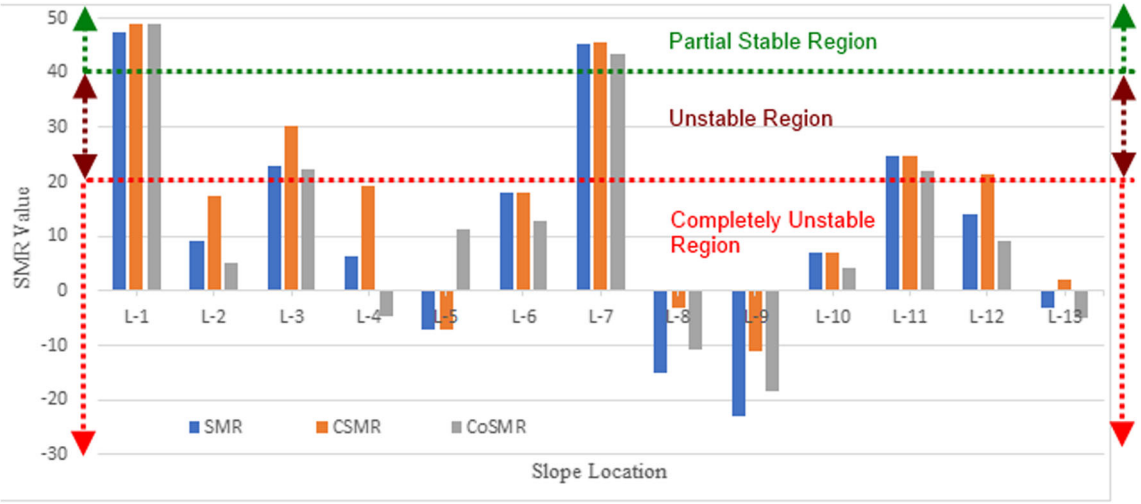

Fig. 8 Comparison between various *SMR* techniques (Original *SMR*, *CSMR* and *CoSMR*)

of *GSI* can also be predicted using the rating of basic *RMR* as given in Eq. 12 (Hoek and Brown 1997). We compared the predicted *GSI* value (GSI_P) and calculated *GSI* value (GSI_C) from the site investigation in Fig. 7. The value of GSI_C ranged from 28 to 58, whereas, for GSI_P, it ranged from 38 to 58. GSI_P was found to be the same as GSI_C for slope L-1, lower for slope L-12 and, for most of the slopes, it was higher than the GSI_C.

$$GSI = RMR_{89} - 5 [for\ GSI \geq 18 \text{ or } RMR_{89} \geq 23] \quad (12)$$

where RMR_{89} is the rock mass rating given by Bieniawski (1989).

Comparison between *SMR*, *CSMR* and *CoSMR*

The various *SMR* techniques, i.e. discrete (Original *SMR* and Chinese *SMR*) and continuous *SMR*, were compared by considering the minimum calculated score from Table 5 to account for the maximum vulnerability for each slope (Fig. 8). In the comparative analysis, a distinguishable difference was observed between discrete *SMR* and continuous *SMR* for most of the slopes. The scores of both discrete *SMR* techniques (i.e *SMR* and *CSMR*) show a slight difference, but their stability class was found to be the same for each slope, except L-12. For slope L-12, *SMR* represents class V whereas *CSMR* represents class IV. The slopes that fall under partially stable and unstable region show a slight difference between scores of *SMR*, *CSMR* and *CoSMR* techniques, whereas for the slopes of a completely unstable region, the difference is higher. The continuous *SMR* scores were found to be lower as compared to discrete *SMR* scores for most of the slopes, which indicates that the maximum vulnerable result was obtained from the continuous *SMR*. Although all three *SMR* techniques have different final scores, their stability class was the same for all the slopes, except L-12. For some of the slopes, both discrete and continuous *SMR* show negative scores, especially in the case of wedge failure, as the joint orientations were very unfavourable. The slopes with negative scores represent class V of the Romana (1985) interpretation.

Conclusion

Engineering Rock Mass Classification Systems provide very important tools for assessing vulnerable slopes that are prone to failure. Thirteen slopes of three studied regions (Lengpui, Phunchawng and Aizawl Zoo) from Aizawl city to Lengpui Airport highway have been investigated for assessment of slope stability using rock engineering classification systems. The rockmasses of road cut slopes varyied from good to fair based on basic *RMR*, and a similar result was observed in the quantified *GSI*. Slope L-1 shows good rockmass quality as it has massive rock blocks. Kinematic analysis identified potential modes of failure and validated the observation of various modes of failure during the field survey of the Lengpui, Phunchawng and Aizawl Zoo areas. Wedge failure was found to be prominent in the Lengpui area and Phunchawng area, whereas both planar and wedge failures were observed in the Aizawl Zoo area in the kinematic analysis. The stability of road cut slopes was obtained by using *SMR*, *CSMR* and *CoSMR*, depending on the type of failure. Both discrete and continuous *SMR* scores indicate that the rockmasses vary from normal to very bad. Negative *SMR* scores have been obtained in discrete as well as continuous *SMR* techniques for slopes such as L-5, L-8, L-9 and L-13. These rock slopes represent class V of the Romana (1985) interpretation, which can be considered as very bad rockmass and completely unstable.

The comparative analysis of (i) kinematic feasibility and basic *RMR* score may conclude that the slope with less RMR_b may always have a high kinematic feasibility. (ii) Predicted and calculated *GSI* value may conclude that the predicted *GSI* values from Hoek and Brown (1997) equation are generally overestimated. (iii) Both discrete (*SMR* and *CSMR*) and continuous *SMR* (*CoSMR*) represents the same stability class for all three regions, except for slope L-12. *CSMR* was found to be less effective, as the height of all studied slopes were less than 80 m. *CoSMR* is based on a continuous function and gives the specific score for each input factor. Maximum vulnerability results were also obtained by *CoSMR* for most of the slopes, which indicates that these slopes need further numerical analysis and proper protective measures.

Acknowledgements The authors would like to thank MOES (Ministry of Earth Sciences, India) for financially supporting this study (MOES/P.O.(GeoSci)/42/2015).

References

Anbalagan R (1992) Landslide hazard evaluation and zonation mapping in mountainous terrain. Eng Geol 32(4):269–277

Anbazhagan S, Ramesh V, Saranaathan SE (2017) Cut slope stability assessment along Ghat road section of Kolli hills, India. Nat Hazards 86(3):1081–1104

Azarafza M, Akgun H, Asghari-Kaljahi E (2017) Assessment of rock slope stability by slope mass rating (*SMR*): a case study for the gas flare site in Assalouyeh, south of Iran. Geotech. Eng. 13(4):571–584

Azzuhry Y (2016) Stability analysis and failure mechanisms of open pit rock slope. J. Civ. Eng. Forum 2(3):141–146

Basahel H, Mitri H (2017) Application of rock mass classification systems to rock slope stability assessment: a case study. J Rock Mech Geotech Eng 9(6):993–1009

Bieniawski ZT (1979) The geomechanical classification in rock engineering applications. In: Proceedings of the 4th International Congress Rock Mechanics, Montreux, Balkema, Rotterdam, vol 2, pp 41–48

Bieniawski, Z. T. (1989). Engineering rock mass classifications: a complete manual for engineers and geologists in mining, civil, and petroleum engineering. John Wiley & Sons

Chaurasia AK, Pandey HK, Nainwal HC, Singh J, Tiwari SK (2017) Stability analysis of rock slopes along Gangadarshan, Pauri, Garhwal, Uttarakhand. J Geol Soc India 89(6):689–696

Chen Z. (1995). Recent developments in slope stability analysis. In: Fujii T, editor. Proceedings of the 8th International Congress of Rock Mechanic, vol. 3; p. 1041–8

Goel, R. K., & Singh, B. (2011). *Engineering rock mass classification: tunnelling, foundations and landslides*. Elsevier., p. 55, 231

Hack, R. (2002). An evaluation of slope stability classification. In *ISRM International Symposium-EUROCK 2002*. International Society for Rock Mechanics

Hoek E, Brown ET (1997) Practical estimates of rock mass strength. Int J Rock Mech Min Sci 34(8):1165–1186

Kaya A (2017) Geotechnical assessment of a slope stability problem in the Citlakkale residential area (Giresun, NE Turkey). Bull Eng Geol Environ 76(3):875–889

Kesari, G. K. (2011). Geology and mineral resources of Manipur, Mizoram, Nagaland and Tripura. Geological Survey of India, 1, 1–103

Kumar N, Verma AK, Sardana S, Sarkar K, Singh TN (2017) Comparative analysis of limit equilibrium and numerical methods for prediction of a landslide. Bull Eng Geol Environ 77(2):595–608

Kundu, J., Sarkar, K., Tripathy, A., & Singh, T. N. (2017). Qualitative stability assessment of cut slopes along the National Highway-05 around Jhakri area, Himachal Pradesh, India. J. Earth Syst. Sci., 126(8), 112

Laldinpuia, Kumar S, Singh TN (2014) 11th may, 2013 Laipuitlang rockslide, Aizawl, Mizoram, north-East India. In: Landslide science for a safer Geoenvironment. Springer, Cham, pp 401–405

Lallianthanga RK, Lalbiakmawia F (2013) Landslide Hazard zonation of Aizawl district, Mizoram, India using remote sensing and GIS techniques. Int. J. Remote Sens. Geosci 2(4):14–22

Liu YC, Chen CS (2007) A new approach for application of rock mass classification on rock slope stability assessment. Eng Geol 89(1):129–143

Marinos P, Marinos V, Hoek E (2007) Geological strength index (*GSI*). A characterization tool for assessing engineering properties for rock masses. Underground works under special conditions. Taylor and Francis, Lisbon, pp 13–21

Palmstrom, A. (1982). The volumetric joint count—A useful and simple measure of the degree of jointing. In IVth International Congress IAEG (pp. V221–V228). New Delhi, India

Pantelidis L (2009) Rock slope stability assessment through rock mass classification systems. Int J Rock Mech Min Sci 46(2):315–325

Rocscience Inc. (2010). Dips, version 5.0. http://www.rocscience.com

Romana, M. (1985). New adjustment ratings for application of Bieniawski classification to slopes. In International Symposium on the Role of Rock Mechanics (pp. 49–53). Zacatecas, Mexico

Sarkar K, Buragohain B, Singh TN (2016) Rock slope stability analysis along NH-44 in Sonapur area, Jaintia hills district, Meghalaya. J Geol Soc India 87(3):317

Siddique T, Alam MM, Mondal MEA, Vishal V (2015) Slope mass rating and kinematic analysis of slopes along the national highway-58 near Jonk, Rishikesh, India. J Rock Mech Geotech Eng 7(5):600–606

Singh, T. N., & Verma, A. K. (2007). Evaluating the slope instability of the Amiya Slide. In 1st Canada-US Rock Mechanics Symposium. American Rock Mechanics Association

Singh AK, Kundu J, Sarkar K (2018) Stability analysis of a recurring soil slope failure along NH-5, Himachal Himalaya, India. Nat Hazards 90(2):863–885

Sonmez H, Ulusay R (2002) A discussion on the Hoek-Brown failure criterion and suggested modifications to the criterion verified by slope stability case studies. Yerbilimleri 26(1):77–99

Tomás R, Delgado J, Serón JB (2007) Modification of slope mass rating (*SMR*) by continuous functions. Int J Rock Mech Min Sci 44(7):1062–1069

Verma AK, Singh TN (2010) Assessment of tunnel instability—a numerical approach. Arab J Geosci 3(2):181–192

Verma AK, Singh TN, Chauhan NK, Sarkar K (2016) A hybrid FEM–ANN approach for slope instability prediction. J. Inst. Eng. (India) Series A 97(3):171–180

Verma AK, Sardana S, Singh TN, Kumar N (2018a) Rockfall analysis and optimized Design of Rockfall Barrier along a strategic road near Solang Valley, Himachal Pradesh, India. Indian Geotech J. https://doi.org/10.1007/s40098-018-0330-6

Verma, A. K., Sardana, S., Sharma, P., Dinpuia, L., & Singh, T. N. (2018b). Investigation of rockfall-prone road cut slope near Lengpui Airport, Mizoram, India. Journal of Rock Mechanics and Geotechnical Engineering

Yardimci AG, Karpuz C (2018) Fuzzy approach for preliminary design of weak rock slopes in lignite mines. Bull Eng Geol Environ 77(1):253–264

Zheng Y, Chen C, Liu T, Xia K, Liu X (2017) Stability analysis of rock slopes against sliding or flexural-toppling failure. Bull Eng Geol Environ:1–21